

PORE-NETWORK MODELING OF ROCK TRANSPORT PROPERTIES: APPLICATION TO A CARBONATE

S. Békri, O. Vizika

Institut Français du Pétrole, 1 et 4 avenue de Bois-Préau, 92852 Rueil-Malmaison, France

This paper was prepared for presentation at the International Symposium of the Society of Core Analysts held in Trondheim, Norway 12-16 September, 2006

ABSTRACT

Network models constructed using different types of pore size distribution have been used to calculate multiphase flow and electrical properties of a homogeneous carbonate. The characteristics of the 3-D pore-network are defined with the requirement that it satisfactorily reproduces the capillary pressure curve, the porosity, the permeability and the formation resistivity factor values, which were determined experimentally. Oil/water capillary pressure, resistivity index and relative permeabilities are calculated and compared to experimentally determined curves. The simulations show that different pore size distributions can lead to similarly good fitting of the experimental capillary pressure, porosity and absolute permeability. However, only the appropriate one satisfies, in addition to these properties, the measured formation resistivity factor. A sensitivity study on the pore-throat size distribution has been performed. The effect of the relationship between formation resistivity factor and permeability on the selection of the pore-throat size distribution, that has to be used to construct the pore network representative of the considered rock, is demonstrated.

INTRODUCTION

The microscopic pore space structure of a porous medium controls fluid transport and electrical characteristics of the reservoir rocks. Therefore, solving the local transport equations in real pore space structure should lead to predictive values for the macroscopic properties (K_r , IR and P_c). Detailed characterization of the pore space geometry and topology incorporated to a pore network model would be necessary to calculate transport properties in a predictive way. Some recent advances in microtomography (Sheppard et al, 2005, Appoloni et al., 2005) will contribute significantly to attain this objective. However, these experiments are very specific and not easy to run on many samples. Besides, they will not be of any help for submicronic porosity. The main idea of the approach presented in this paper is to provide a simple geometry 3D network in which flow calculations can be made. This network is not an exact representation of the pore space; however it contains significant pore structure information such as connectivity and pore size distribution. Also it accounts for various flow and displacement mechanisms occurring at the pore scale. This modeling permits the calculation of different petrophysical parameters relevant for single phase or multiphase flow (e.g. absolute permeability, relative permeabilities of fluids, formation factor, electrical resistivity index, etc.). An extended review of most of pore network models is given by Sahimi (1993), while significant efforts have been made more recently for the prediction of

macroscopic transport coefficients of the real rocks using pore network models (Oren, 2002).

The pore network modeling technique presented in this paper relies on the construction of the network (pore and throat size distributions, aspect ratios, pore-to-pore lengths) such that it fits standard macroscopic parameters of the rock. It has been shown previously (Laroche & Vizika, 2005) that fitting the mercury P_c , the porosity and the permeability does not guarantee uniqueness of the solution (e.g. does not constrain the network model sufficiently to be predictive in the transport properties calculations).

In the present work it is shown that, for a given wettability, information on the formation factor -in addition to P_c , K and ϕ - is sufficient to constrain the problem and to reproduce the experimental results of resistivity index curve (IR) and the oil/water relative permeabilities (Kr). The investigated rock is a homogeneous unimodal carbonate rock with a porosity of 34.1% and permeability of 2.7 mD. The resistivity index curve and the oil/water relative permeabilities are calculated for this network and compared to experimental curves. The key features of the model giving the most representative pore network are stressed out. The effect of input parameters on the prediction of IR and oil/water Kr of homogeneous media is discussed.

PORE-SCALE MODELING

Network Model Construction

Pore Space Features

A network model of the pore-and-throat type is a conceptual representation of a porous medium. Although it does not describe the exact morphology of a porous medium, it is able to take into account essential features of the pore space geometry and topology (Thauvin et al., 1998). The network model developed in this work respects the converging-diverging nature of pores, the pore space multiple connectivity, the pore-size distribution and the existence of pore space angulosities. The pore space is simulated as a three-dimensional cubic lattice formed by pore-bodies (nodes) interconnected by pore-throats (bonds), as shown in Figure 1. The coordination number (bonds per node) can be varied. Here it is taken equal to 6, but it can take any value between 1 and 6. More details on the model characteristics and construction are provided in a previous paper (Laroche and Vizika, 2005).

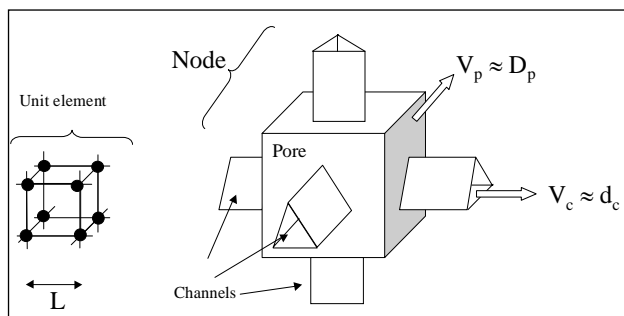


Figure 1: Schematic depiction of a unit cell of the network model (Laroche and Vizika, 2005)

Pore Network Parameters

In the simulations presented here each pore-body is assumed to be accessible by six pore-throats of identical inscribed diameter d . This implies that pore-throats, which link by definition two pore-bodies, do not have a constant section and are defined by two diameters. The aspect ratio, AR , relates the pore-body diameter D , to the pore-throat diameter d . The pore-body volume is assumed to be proportional to the pore inscribed diameter D to a certain exponent, λ_p , following the relationship $V_p(D) \sim D^{\lambda_p}$. This empirical approach has been used by many authors to represent the relationship between radius and volume for real pores (Heiba et al., 1992; Fenwick and Blunt, 1998). Here the relationship for the pore-body volume is identical to $V_p(d) \sim (ARd)^{\lambda_p}$, since in the present work D and d are correlated through the aspect ratio AR . More precisely:

$$V_p(d) = C_p \bar{D}^{(3-\lambda_p)} AR^{\lambda_p} d^{\lambda_p} \quad (1)$$

where C_p is a coefficient approximately equal to $(\phi.L^3 / \bar{D}^{(3-\lambda_p)} \bar{D}^{\lambda_p})$, ϕ is the porosity, L is the lattice periodicity length (node-to-node distance) and \bar{D} the average pore-body diameter. The pore-throat length, l_t , is assumed to be correlated to the pore-throat radius according to three different scenarios. It can be considered as constant, proportional or inversely proportional to the pore-throat radius depending on the value of λ_t :

$$\begin{cases} lt_{\lambda_t} = C_t \cdot (L - \bar{D}) \cdot (d/\bar{d})^{\lambda_t} , & \text{for } \lambda_t = 0, 1 \\ lt_{-1} = C_t \cdot (L - D) & , \text{for } \lambda_t = -1 \end{cases} \quad (2)$$

The prefactor C_t in the relationships (2) is a coefficient that has to be tuned to fit the permeability. For a given λ_p and pore throat distribution, C_p , C_t and L are adjustable parameters that permit to reproduce the rock permeability, porosity and formation resistivity factor obtained experimentally.

The porosity is given as a function of the adjustable parameters and the pore/throat distribution by the following equations:

$$\begin{cases} \phi_1 = C_p \cdot L^{-3} \cdot \bar{D}^{(3-\lambda_p)} \cdot \bar{D}^{\lambda_p} + 1/2 \cdot Z \cdot C_t' \cdot \bar{d}^3 \cdot L^{-3} , \\ \phi_0 = C_p \cdot L^{-3} \cdot \bar{D}^{(3-\lambda_p)} \cdot \bar{D}^{\lambda_p} + 1/2 \cdot Z \cdot C_t' \cdot \bar{d} \cdot \bar{d}^2 \cdot L^{-3} , \\ \phi_{-1} = C_p \cdot L^{-3} \cdot \bar{D}^{(3-\lambda_p)} \cdot \bar{D}^{\lambda_p} + 1/2 \cdot Z \cdot C_t' \cdot \bar{d}^3 \cdot \frac{(L - D) \cdot d^2}{(L - \bar{D}) \cdot \bar{d}^2} \cdot L^{-3} \end{cases} \quad (3)$$

where ϕ_{λ_t} is the porosity for different λ_t or different scenarios for the pore-throat length, Z is the coordination number and C_t' is equal to $C_t \cdot (L - \bar{D}) / \bar{d}$.

The absolute permeability and the formation resistivity factor of the network cannot be related analytically to the adjustable parameters and the pore/throat distribution as done for the porosity in equation 3. However, for a bundle of capillary tubes characterized by a given distribution of diameters and a length defined by equation 2, simple relations can be derived for the absolute permeability and formation resistivity factor as:

$$\left\{ \begin{array}{l} K_{//1} \cong C_t'^{-1} \cdot L^{-1} \cdot \overline{d^3}, \\ K_{//0} \cong C_t'^{-1} \cdot L^{-1} \cdot \overline{d^{-1}} \cdot \overline{d^4}, \\ K_{//1} \cong C_t'^{-1} \cdot L^{-1} \cdot \overline{d^{-1}} \cdot \left[\frac{(L-D)}{(L-D)} d^4 \right] \end{array} \right. \quad \text{and} \quad \left\{ \begin{array}{l} FF_{//1} \cong C_t' \cdot L \cdot \overline{d^{-1}}, \\ FF_{//0} \cong C_t' \cdot L \cdot \overline{d^{-1}}, \\ FF_{//1} \cong C_t' \cdot L \cdot \overline{d^{-1}} \cdot \left[\frac{(L-D)}{(L-D)} d^2 \right]^{-1} \end{array} \right. \quad (4)$$

It is interesting, in this case, to evaluate the product $\{FF.K\}$. It is found to depend only on the pore-throat size distribution:

$$FF_{//1} \cdot K_{//1} \cong \frac{\overline{d^3}}{d}, \quad FF_{//0} \cdot K_{//0} \cong \frac{\overline{d^4}}{d^2}, \quad FF_{//1} \cdot K_{//1} \cong \frac{\overline{d^4 / (L-D)}}{d^2 / (L-D)} \quad (5)$$

Pore Size Distribution

In network modeling the identification of size distributions for pore bodies and pore throats is a very challenging task. The Pc - S curve can be converted into r vs. S curve, where r is the pore radius, assuming that Pc across the interface is given by the Young-Laplace equation. These data are usually interpreted in a conventional way to obtain pore size distributions. The main assumption is the absence of interconnectivity between pores, implying that the pores are occupied by mercury progressively from the bigger to the smaller and at each pressure step all the occupied pores have the same size. The number based throat size frequency can be determined by assuming that: (i) radii r calculated from the capillary pressure values correspond to the threshold radii to invade pore bodies of radius $R \sim r$ and (ii) the elementary volume of a pore (a node and its throats) follows $v(r) \sim r^{\lambda_p}$. The number based frequency is given by:

$$F_{//n}(r) = \left| \frac{\langle v \rangle}{v(r)} dS \right| \quad (6)$$

where $\langle v \rangle$ is the average elementary volume of a pore. The extracted pore size distribution from mercury injection corresponds to a model of the type bundle of capillary tubes. If this pore size distribution is injected into a network model, the simulated Pc - S curve will not fit the experimental Pc - S values. In the case of a 3D connected network, the mercury interpretation tends to underestimate the number of large pore-throats since, in real media, they can be surrounded by small pore-throats and thus their volume is attributed to the smallest pore-throats.

The approach that is used in this work consists in inverting the mercury capillary pressure curve first, then in modifying the obtained pore size distribution until the constructed network fits the P_c - S curve. In fact to construct a 3D interconnected pore network, the pore size distribution extracted from the conventional interpretation of the mercury injection is used as a first guess, then it is tuned manually to derive the required one that satisfactorily reproduces the experimental capillary pressure curve. Note that in this work the pore-body size is assumed to be proportional to its threshold radius $R \sim r$ through the aspect ratio AR . Thus, the pore-throat size distribution will determine the pore-body size distribution automatically.

In an early work, pore throat and the pore body sizes were assumed to follow a given distribution (Weibull distributions (Ioannidis and Chatzis, 1993)). The Weibull cumulative density function is generally defined as follows:

$$F_i(r_i) = 1 - \exp \left[- \left(\frac{r_i - r_i^{\min}}{\alpha_i} \right)^{\beta_i} \right] / 1 - \exp \left[- \left(\frac{r_i^{\max} - r_i^{\min}}{\alpha_i} \right)^{\beta_i} \right], \quad i = \text{pore throat, pore body} \quad (7)$$

where α_i , β_i are parameters of the distributions. The minimum and maximum pore size (r_i^{\min} , r_i^{\max}) can be extracted for the pore throat from the mercury injection P_c curve. As it will be seen below, Weibull distribution approximates satisfactorily the manually determined pore size distribution. It will be preferred in this paper to the latter one, in order to simplify calculations and comparisons.

Calculation of the Network Petrophysical Parameters

Network Invasion Methodology

The P_c curve is obtained by simulating quasi-static displacement. An increasing pressure is applied on the injected fluid while the pressure of the fluid in place is kept constant. During quasi-static displacement, viscous pressure gradients are negligible and the pressure of each phase is constant everywhere within the network. Expressions to evaluate the saturations in each unit element can be found elsewhere (Laroche and Vizika, 2005).

Relative Permeability and Resistivity Index Calculation

The absolute permeability K of the network is found from Darcy's law when the network is fully saturated with a single phase. The two-phase relative permeability curves are calculated at each step of the two-phase quasi-static displacements when capillary equilibrium is reached. Flow within each phase is simulated by applying a macroscopic pressure gradient ΔP across the network of length L_{net} , and by solving for the local pressure at each pore body. If Q_α is the flow rate, μ_α the viscosity of phase α , K the permeability and A the cross-section of the porous medium, the relative permeability of phase α is calculated as:

$$K_{r\alpha} = \frac{Q_{\alpha} \mu_{\alpha} L_{net}}{AK\Delta P} \quad (8)$$

The electrical analogy to absolute permeability is the formation factor

$$FF = \sigma_w / \sigma_0 \quad (9)$$

where σ_0 is the electrical conductivity computed at 100% water saturation and σ_w is the electrical conductivity of bulk water. The network conductivity is given by Ohm's law

$$\sigma_0 = \frac{I.L_{net}}{A.\Delta V} \quad (10)$$

where ΔV is the imposed voltage and I is the total current intensity. The equations are solved for the potential at each node, imposing current conservation at every pore body. The electrical resistivity index IR is given by

$$IR = \sigma_0 / \sigma_t \quad (11)$$

where σ_t is the electrical conductivity at a given water saturation.

Potential and Pressure Field Calculation

The calculation of the fluid flow of each phase spanning the network and the calculation of the electrical current in the aqueous phase each use the same electrical analog. Electrical and hydraulic conductivities are used to solve for the potential and pressure field, respectively.

The local electrical conductance, g_{eij} , relates the local electrical flux, I_{ij} , between two neighboring pores, ij , to the potential difference between these two pores:

$$I_{ij} = g_{eij} (U_i - U_j) \quad (12)$$

This equation only applies to the electrically conductive phase, i.e. the water phase. Similarly, for laminar flow the relationship between pressure drop and fluid flux in the network is linear. The local flow rate for a given phase α between pore i and neighboring pore j is defined as:

$$q^{\alpha}_{ij} = g^{\alpha}_{ij} (P^{\alpha}_i - P^{\alpha}_j) \quad (13)$$

where g^{α}_{ij} is the local hydraulic conductance of the particular fluid α , in bulk phase or in films between pores i and j . In each pore i , the continuity equations are verified. Electrical and hydraulic problems are reduced to a system of linear algebraic equations the solution of which gives respectively the electrical potential and pressure of each phase in the pores.

The electrical conductance of the water phase in a pore segment of length l is given by:

$$g_e = \sigma_w A_w / l \quad (14)$$

where A_w is the cross-sectional area occupied by the water phase. The calculation of the effective electrical conductance between two neighboring pores takes into account the water phase occupancy in the different pore segments (pores and throat). Expressions for the hydraulic conductance of a wetting or a non-wetting phase in a pore can be found in a previous paper (Laroche and Vizika, 2005).

RESULTS AND DISCUSSION

Network Construction

Pore network models have been constructed using manually fitted pore-throat size distribution and Weibull function (Figure 2). The parameters of the pore network model are set constant for all the runs ($L=70 \mu\text{m}$, $AR=4$, $\lambda_t=1$) and the prefactors C_p and C_i are tuned to fit the target porosity and permeability of the investigated rock (homogeneous carbonate with $\phi=34.1\%$, $K=2.7\text{mD}$ and $FF=7.54$). The pore-throat size distribution extracted directly from mercury interpretation is compared to the tuned one named "manual fitting" in Figure 2.a. The Weibull distribution also fitting the experimental oil/water capillary pressure is given in the same figure.

Figure 2.c shows that when the pore network is constructed with the pore size distribution obtained from the conventional interpretation of the mercury P_c , the simulated capillary pressure does not fit the experimental values. This was expected, since the conventional interpretation of the mercury P_c curve is based on the hypothesis that the porous medium is a bundle of parallel and non communicating capillary tubes. Injecting this pore size distribution in a network model that introduces features (interconnectivity, aspect ratio) non existing in the bundle of capillaries model lead to calculation that cannot fit the experimental results. This conventional pore size distribution can be used only as a first guess and has to be adjusted until the experimental P_c - S curve is fitted.

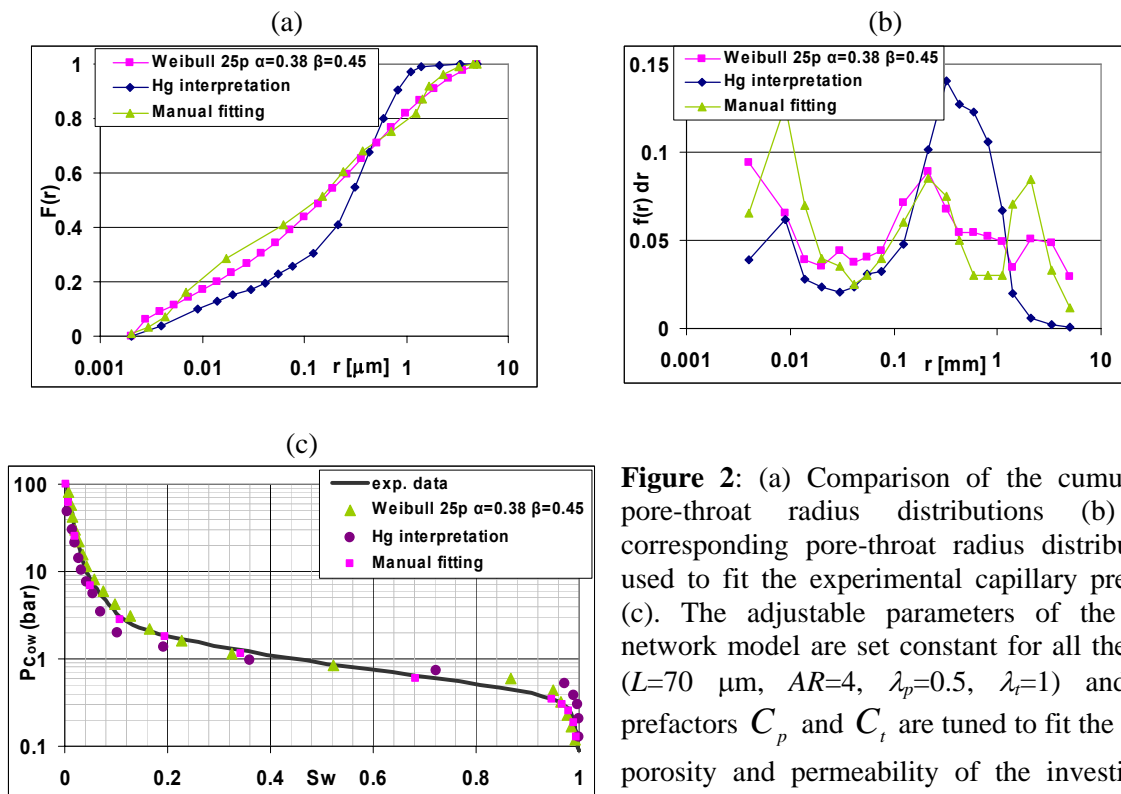


Figure 2: (a) Comparison of the cumulative pore-throat radius distributions (b) the corresponding pore-throat radius distributions used to fit the experimental capillary pressure (c). The adjustable parameters of the pore network model are set constant for all the runs ($L=70 \mu\text{m}$, $AR=4$, $\lambda_p=0.5$, $\lambda_t=1$) and the prefactors C_p and C_i are tuned to fit the target porosity and permeability of the investigated rock ($\phi=34.1\%$ and $K=2.7\text{mD}$).

Figure 2.b shows that the conventional mercury interpretation underestimates the largest and the smallest pore-throats. This is attributed to the fact that in real rocks large pore-throats can be surrounded by smaller pore-throats. As a consequence large pore-throats may be invaded at pressures higher than their corresponding pressures. Thus their volume will be attributed to smaller pore-throats. This will increase the number of the intermediate size pore-throats and consequently reduce the number of the largest and the smallest ones.

Figure 2.a shows also that the tuned pore-throat size distribution can be represented by a Weibull distribution ($\alpha = 0.38$ and $\beta = 0.45$, for the present case). To simplify calculations and comparisons Weibull distributions will be used in the remaining of the paper.

Calculated oil/water capillary pressure curves presented in Figures 2.c and 3.a have been obtained by simulating oil invasion in these water-wet network models initially fully saturated with water. Comparison with the experiment (Figure 3.a) shows that a very good fit of the oil/water capillary pressure can be obtained with different pore-throat size distributions (i.e. different λ_p), although different values of the formation resistivity factor are obtained (see Table 1). It is reminded here that the experimentally determined FF value is 7.54 which best corresponds to the result of run with $\lambda_p=0.55$.

Table 1. Calculated formation resistivity factor FF for different pore-throat radius distributions that fit the experimental porosity, permeability and capillary pressure.

Hg interp. with $\lambda_p=0.5$ manual fitting $FF = 8.8$	Weibull 25p with $\lambda_p=0$. $\alpha=0.6 \beta=1.1$ $FF = 16.1$	Weibull 25p with $\lambda_p=0.5$ $\alpha=0.38 \beta=0.45$ $FF = 8.6$	Weibull 25p with $\lambda_p=0.55$ $\alpha=0.35 \beta=0.4$ $FF = 7.5$
---	---	--	--

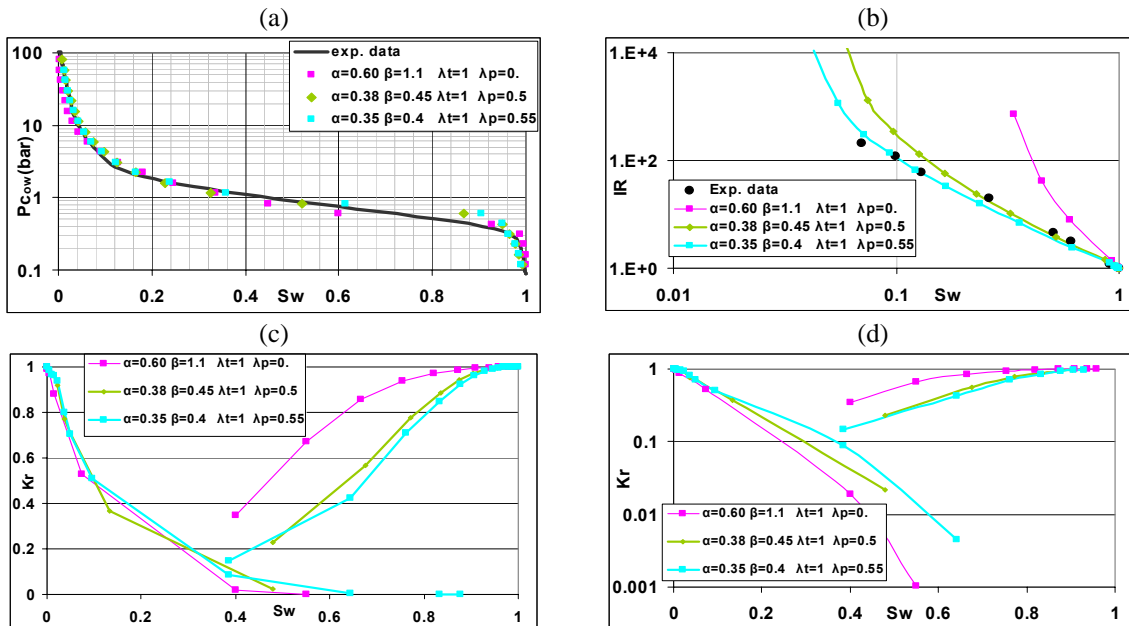


Figure 3: Comparison between experimental and calculated curves: (a) oil-water capillary pressure (b) resistivity index. Calculated oil and water relative permeabilities (c and d). The pore network models have been constructed using the different scenarios described in Table 1

Resistivity Index

The resistivity index (*IR*) for drainage of a water-wet rock has been simulated, as for the capillary pressure by oil invasion in water-wet network, and compared to the experimental results. Figure 3.b shows a good agreement with the experiment for the case where the pore-body volume is assumed to be proportional to the inscribed pore diameter *D* to an exponent $\lambda_p=0.55$ and where the pore-throat length was supposed to be proportional to the pore-throat radius ($\lambda_t=1$). This case is the one for which the best agreement is obtained for the formation resistivity factor *FF* between measurement and calculation (Table 1) with a difference of less than 1%.

Relative Permeabilities

Oil/water relative permeabilities for forced imbibition have been calculated by simulating water invasion in oil-wet networks. Networks are constructed using the pore-throat size distribution that fits oil/water pressure obtained with the different scenarios described in Table 1. The results are presented in Figures 3.c and 3.d both in linear and logarithmic coordinates. The figure shows how relative permeabilities are affected by the correlation between the pore volume behind each throat and its radius.

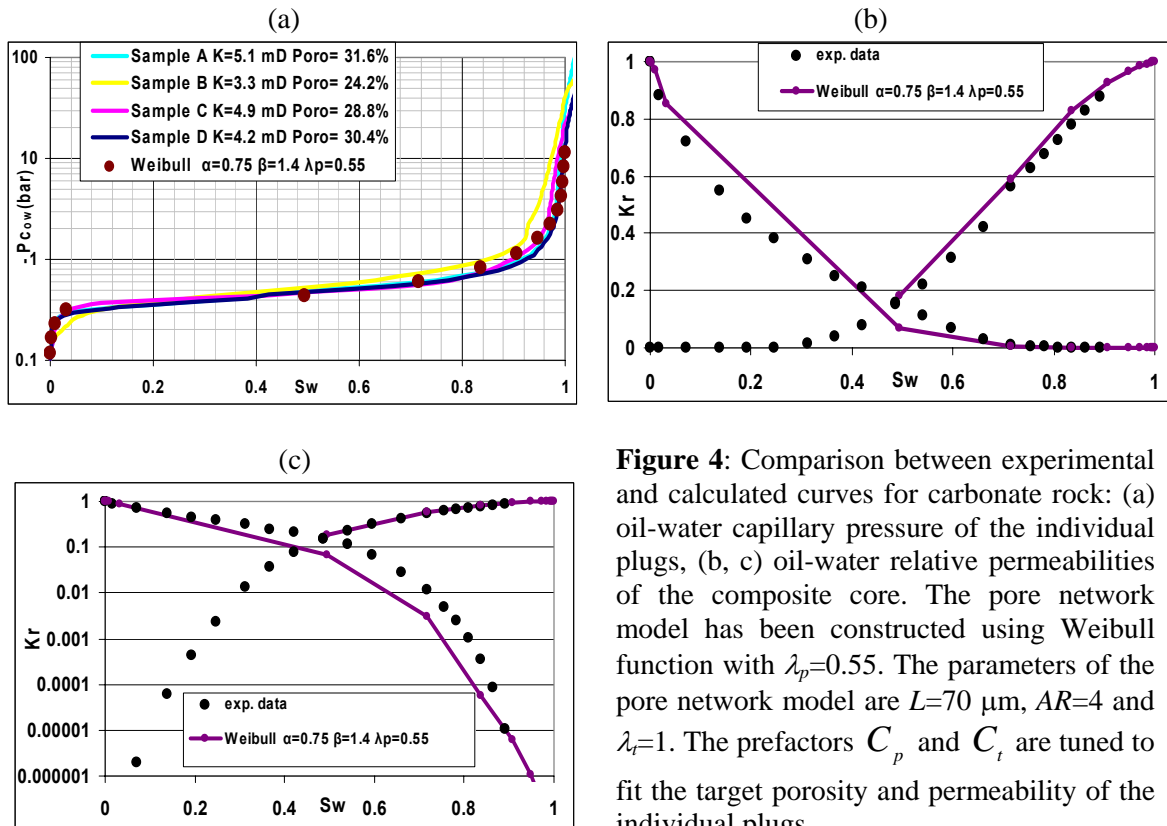


Figure 4: Comparison between experimental and calculated curves for carbonate rock: (a) oil-water capillary pressure of the individual plugs, (b, c) oil-water relative permeabilities of the composite core. The pore network model has been constructed using Weibull function with $\lambda_p=0.55$. The parameters of the pore network model are $L=70 \mu\text{m}$, $AR=4$ and $\lambda_t=1$. The prefactors C_p and C_t are tuned to fit the target porosity and permeability of the individual plugs.

Unsteady State oil/water relative permeabilities have been determined experimentally in a restored wettability composite of four sister plugs of the above considered carbonate rock. The data have been numerically interpreted with full account of capillary end effects. The experimental oil/water Pc for each plug of the composite and Krs of the composite core are given in Figure 4 and compared to the simulated ones. A good agreement between calculated and experimental values is obtained for the pore network model corresponding to the case that gives the best agreement with the measured formation resistivity factor, FF (Table 1, $\lambda_p = 0.55$).

Effect of Weibull Parameters (α and β)

In order to investigate the effect of the pore-throat size distribution on the petrophysical parameters, we constructed pore-network models with the Weibull distribution with different α and β parameters. In all the simulations (shown in Figures 5 and 6) the porosity and the absolute permeability have been fitted to the experimental values ($\phi=34.1$, $K=2.7$ mD). The parameter β is related to the width of the pore-throat distribution (Figure 5). Increasing β leads to narrower pore size distributions. It is seen in Figure 6 that β has small effect on the capillary pressure curve and saturation exponent for high water saturations. However, it affects the resistivity index curves at low water saturation.

The parameter α , which is related to the location of the maximum of the pore-throat distribution (Figure 5), affects strongly the capillary pressure curve. The higher the value of α the lower the breakthrough capillary pressure is (Figure 6.a). α affects also strongly both the resistivity index and the saturation exponent. The higher the value of α the lower the saturation exponent n is (Figure 6.c). The "non-Archie" behavior of the IR curves at low saturation (Figure 6.d) is related to the value of β or rather to the width of the pore-throat distribution as it was explained in previous work (Bekri et al., 2005).

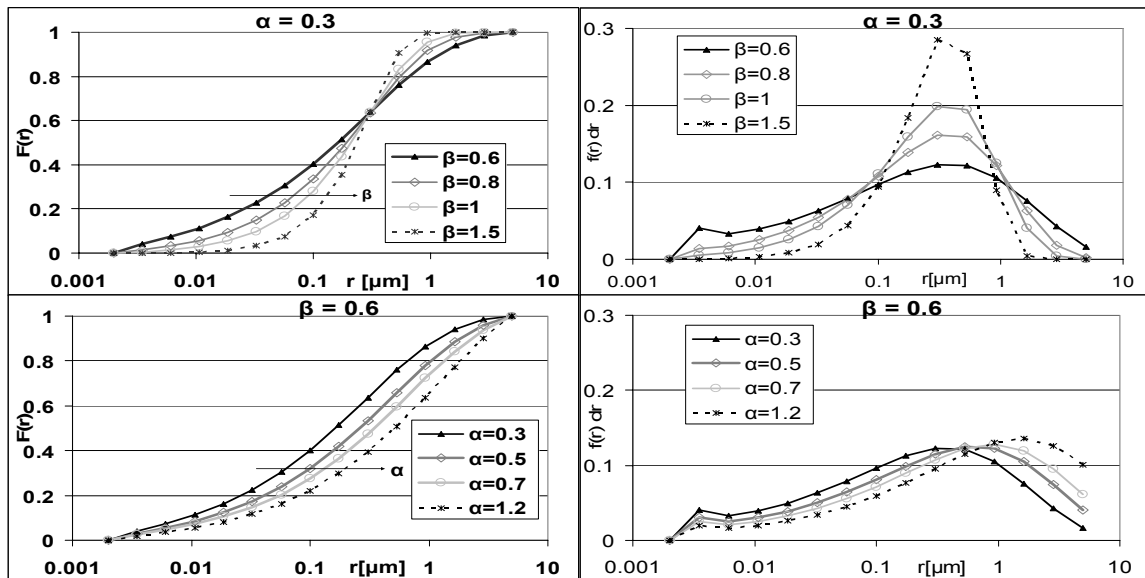


Figure 5: Weibull pore-throat radius distributions obtained with different β and α scenarios.

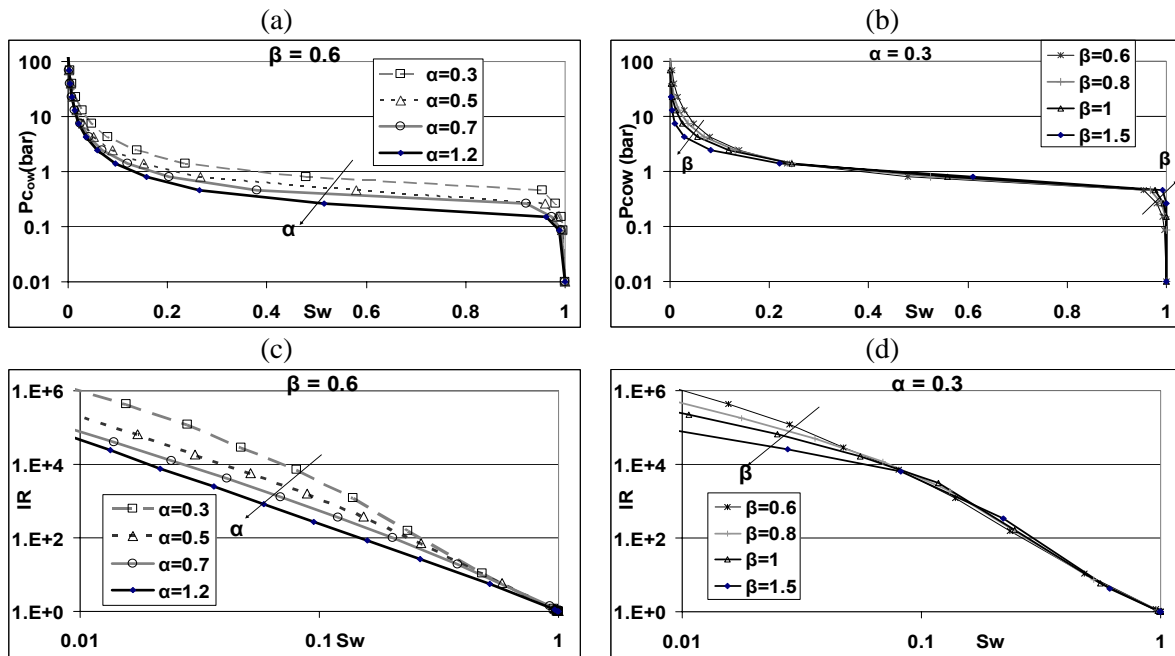


Figure 6: Effect of the Weibull parameters α and β on the simulated oil-water capillary pressure curves (a, b) and simulated resistivity index curves (c, d). The parameters of the network model are set constant for all the runs ($L=25 \mu\text{m}$, $AR=2$, $\lambda_p=0.5$, $\lambda_t=0$). The prefactors C_p and C_i are tuned to fit the target porosity (34.1%) and permeability (2.7 mD).

Finally, the formation resistivity factor FF is mapped in Figure 7. It is clear from this figure that, for a given permeability, the formation resistivity factor depends on both parameters α and β of the Weibull function, even though it is more sensitive to the average pore-throat size (reflected by α) than to the width of the pore size distribution (reflected by β). Nevertheless it contains information on the pore structure that is complementary to the one of permeability or capillary pressure. Thus it should be used along with these properties to select the most representative pore network for further transport calculations.

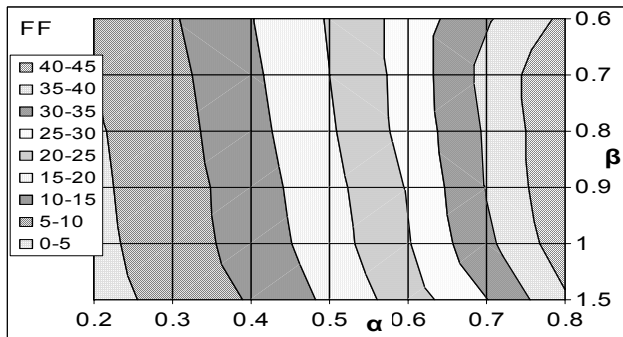


Figure 7: Calculated formation resistivity factor FF as a function of the Weibull parameters α and β . The other parameters are the same as in Figure 6.

CONCLUSIONS

Network modeling has been used to construct pore networks satisfying capillary and standard petrophysical properties of a homogeneous carbonate rock. Oil/water relative permeabilities and resistivity index have been calculated for these networks and compared to experimentally determined curves.

The simulations confirm previous observations, that reproducing the experimental porosity, absolute permeability and capillary pressure curve is not sufficient to characterize the transport properties in a predictive way. Information on the formation resistivity factor would be necessary to better constrain the problem. The comparison between experimental and calculated values indicates that reproducing the formation factor would be also sufficient to get predictive values for the resistivity index and the relative permeabilities. This observation has to be validated more extensively.

Detailed microtomography studies will bring new insight in the understanding of the effect of pore scale structure on the macroscopic properties, and they will permit to validate the above observations.

ACKNOWLEDGEMENTS

The authors wish to thank J.M. Lombard and M. Fleury for providing the experimental data.

REFERENCES

1. Appoloni, C. R., Rodrigues, C. R. O. and Fernandes, C. P., "Porous microstructure characterization of a sandstone reservoir using high-resolution x-ray microtomography", SCA2005-41, *International Symposium of the Society of Core Analysts*, Toronto, 2005.
2. Bekri, S., Laroche, C., Vizika, O., "Pore network models to calculate transport and electrical properties of single or dual-porosity rocks", SCA2005-35, *International Symposium of the Society of Core Analysts*, Toronto, 2005.
3. Fenwick, D.H. and Blunt, M.J., "Three-dimensional modeling of three-phase imbibition and drainage", *Adv. Water Resources*, (1998) **21**(2), 121-143.
4. Heiba, A.A., Sahimi, M., Scriven, L.E. and Davis, H.T., "Percolation theory of to-phase relative permeability", *SPE Reservoir Engineering*, (1992) **7**, 123-132.
5. Ioannidis, M. A. and Chatzis, I., "Network modelling of pore structure and transport properties of porous media", *Chemical Engineering Science*, (1993) **48**, N5, 951-972.
7. Laroche, C., Vizika, O., "Two-Phase Flow Properties Prediction from Small-Scale Data Using Pore-Network Modeling", *Transport in Porous Media*, (2005) **61**, N1, 77-91.
8. Øren, P.E., and Bakke, S., "Process Based Reconstruction of Sandstones and Prediction of Transport Properties", *Transport in Porous Media*, (2002), **46**, 311-314.
9. Ransohoff, T. C. and Radke, C. J., "Laminar flow of a wetting liquid along the corners of a predominantly gas occupied non circular pore", *J. Coll. Interface Sci.*, (1988) **121**, N2.
10. Sahimi, M., "Flow phenomena in rocks: from continuum models to fractals, percolation, cellular automata and simulated annealing", *Rev. Mod. Phy.* (1993) **65**, 1393-1534.
11. Sheppard, A. P., Sok, R. M. and Averdunk, H., "Improved pore network extraction methods", SCA2005-20, *International Symposium of the Society of Core Analysts*, Toronto, 2005.
12. Thauvin, F., Mohanty, K.K., "Network modeling of non-Darcy Flow Through Porous Media", *Transport in Porous Media* (1998) **31**, 19-37.